Interaction of the Monsoon and Pacific Trade Wind System at Interannual Time Scales. Part II: The Tropical Band

T. P. BARNETT

Climate Research Group, Scripps Institution of Oceanography, University of California, San Diego, La Jolla, CA 92093

(Manuscript received 19 March 1983, in final form 29 February 1984)

ABSTRACT

This is the second of three papers describing the interaction between the Monsoon System and the Pacific Trade Wind fields. The current study concentrates on the tropical band within ±30° of the equator; an earlier study (Part I) concentrated on the region ±10° of the equator.

The results of the current study show that the two wind systems are strongly coupled across the tropical latitudes at interannual time scales with coherent variations apparent in the surface wind field from Africa to South America. It appears that the equatorial regions are coupled most strongly to the Southern Hemisphere. The couplings and interaction between the two systems are dependent on the phase of the annual cycle. The apparent temporal bimodality observed in Part I in the near-equatorial band is no longer seen when the full tropical band is analyzed. There is only a slight preference in the wind system for anomalous convergence over Indonesia. The eastward propagation of anomalous zonal wind in the equatorial region is still evident in this analysis.

The results suggest that the atmosphere changes its state in a way that is only broadly related to changes in the sea surface temperature (SST) in the central Pacific. Thus it appears that mechanisms other than those associated with the Pacific SST may be required to explain much of the variability described in this paper. It also appears that the climatic signal being described here is but part of an even larger mode of climatic variability.

1. Introduction

An earlier study investigated the interaction of the Monsoon–Trade Wind system in the zone within ±10° of the equator (Barnett, 1983; hereafter referred to as Part I). The current paper expands the area of investigation to include the zone ±30° of the equator. This extension makes it possible to investigate connections between the midlatitudes and the equatorial zone, and to test the sensitivity of the analysis techniques and results of Part I to a significant variation in geometry (cf. Buell, 1979).

The general arrangement and illustrations of this paper will be as close to Part I as possible to facilitate comparison. The text will not dwell on similarities between Part I and this paper (Part II) other than to point out that they occur and to refer the reader to I. Further, attention will be focused largely on the analysis of the vector wind with reference to the analysis of the individual components only where necessary. With these points in mind, the following sections discuss the data and analyses methods and then the results of analyzing the vector wind components of the monsoon/trade wind field. The last section summarizes the conclusions. A final paper (Barnett, 1984; hereafter referred to as Part III) will attempt to synthesize the results of Parts I and II into a physical scenario for large-scale air–sea interactions in the tropical Indo–Pacific region.

2. Methods

Ship-of-opportunity observations from the Indian Ocean were used to develop a history of the wind field over that ocean from 1950–78. These data were gridded into 2° latitude by 10° longitude quadrangles and averaged over bimonthly time intervals, e.g., bimonth 1 = January plus February. The Indian Ocean winds were merged with the Wyrtki–Meyers (1975) trade wind data for the Pacific; the later set being projected onto a similar space–time grid. The final data set provided coverage between ±30° of the equator from Africa to South America. Examples of the resulting long-term mean fields for selected bimonths are shown in Fig. 1.

Data sparsity in the Pacific makes the series effectively begin in 1952; it extends to 1978. Data gaps were filled by simple objective mapping procedures. These gaps occurred most frequently in the southeast and central equatorial Pacific. Data coverage in the Indian Ocean was generally excellent.

The gridded wind data were next subjected to a complex empirical orthogonal function (CEOF) analysis. The virtue of this method is that it allows detection of large-scale coherent propagating features in the data set in the presence of high noise levels and possible nonstationary situations. This approach, since it can be used to recover information on the cyclostationary character of the data field, was pre-

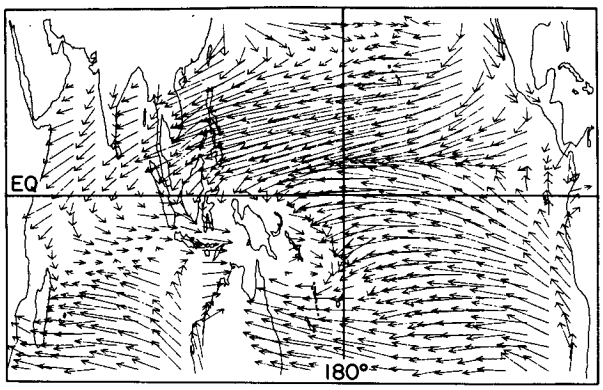

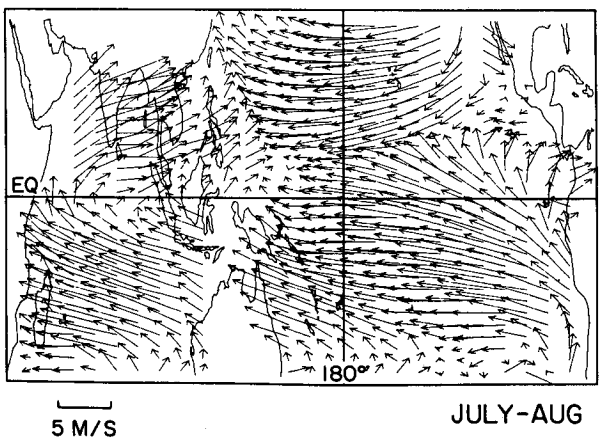

FIG. 1. Seasonal cycle for selected bimonths derived from original data.

ferred over normal cross-spectral analysis. Indeed, strong phase-locking of wind anomalies to the annual cycle (cyclostationary effect) was found in Part I, thereby suggesting the appropriateness of the CEOF approach.

The CEOF method goes as follows: A complex data set U is constructed having as its real part a given data set u and as its imaginary part the Hilbert transform of u. Now U carries the equivalent of both co- and quadrature information on the temporal phase of fluctuations in u so the covariance matrix, $\mathbf{C}_{ij} = (U_i^* U_j)_t$, between spatial locations (i, j) can be used to investigate propagating features in u. Note that the seasonal cycle is removed from U prior to calculating $\mathbf{C}_{ij}$.

The largest eigenvalues of $\mathbf{C}_{ij}$ and its associated eigenvectors define the largest spatially coherent "signals" present in the data. The CEOFs, which are complex but otherwise quite similar to standard EOF analyses, readily give measures of the data field that describe the spatial distributions of energy S_n and time-averaged phase θ_n, i.e., wave number. They also provide a measure of temporal phase ϕ_n, e.g., instantaneous frequency, and a measure of the time modulation of fixed spatial patterns of variability R_n. These latter two time domain measures are useful for detecting the occurrence of cyclostationary effects which might be obscured by normal cross-spectral analysis. The four field measurements discussed above are defined as follows.

$$\text{Spatial phase:} \quad \theta_n(\mathbf{x}) = \arctan\left[\frac{\mathrm{Im}B_n(\mathbf{x})}{\mathrm{Re}B_n(\mathbf{x})}\right]; \quad (1)$$

$$\text{spatial amplitude:} \quad S_n(\mathbf{x}) = [B_n(\mathbf{x})B_n^*(\mathbf{x})]^{1/2}; \quad (2)$$

$$\text{temporal phase:} \quad \phi_n(t) = \arctan\left[\frac{\mathrm{Im}A_n(t)}{\mathrm{Re}A_n(t)}\right]; \quad (3)$$

$$\text{temporal amplitude:} \quad R_n(t) = [A_n(t)A_n^*(t)]^{1/2}; \quad (4)$$

where the $B_n(\mathbf{x})$ are the complex eigenvectors of $\mathbf{C}_{ij}$ and the $A_n(t)$ are the associated principal components.

3. Vector field

The (u, v) components were combined according to (A7) of Part I. The CEOF analysis on the combined data set then described the covariability between the components that may be interpreted as variations in the vector wind. The first four modes (22%) were deemed nonnoise according to Rule N given in Preisendorfer *et al.* (1981). Again, the first mode (35% of the signal) will be discussed, as only its eigenvalue was distinct (cf. North *et al.*, 1982).

The relatively smaller average variance associated with this mode, as opposed to its value in Part I, might be expected: the data fields now extend outside the steady trade wind zones, and the winds at higher latitudes, particularly in the Southern Hemisphere, are not well sampled. However, the average variance is somewhat misleading because the first mode can on occasion account for 64% of the field variance (cf. Section 3b).

a. Spatial properties

The spatial characteristics of the vector field are viewed via the spatial state vector described in Part I and via the spatial amplitude functions. In particular we will investigate the contribution of each component to these variables. (see Appendix Section 3 of Part I). The vector field is obtained by joining the u and v fields so that the original spatial grid of, say, NP points is effectively doubled in size to 2NP. The resulting eigenvectors have 2NP components; the first set of NP components being associated with the u-variability and the second with the v-variability.

The contribution of u- and v-components to variation in the vector field are summarized in Fig. 2. The vector field is dominated by the u-component in

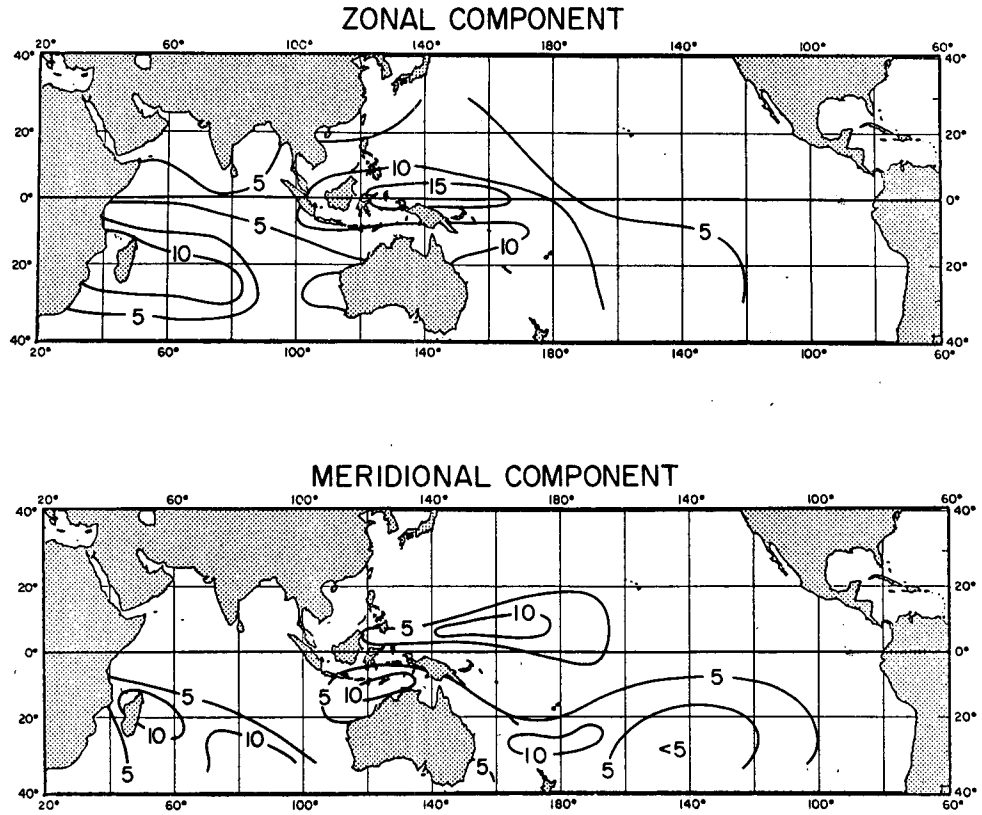

FIG. 2. Top panel shows distribution of spatial amplitude for first empirical mode of the vector wind: zonal component (relative units); lower panel gives distribution of spatial amplitude for first empirical mode of the vector wind: meridional component.

the western equatorial Pacific. The signal weakens as one progresses southeast into the South Pacific. Much the same distribution of energy was found in the *u*-only analysis (not shown). The main contributions from the *v*-component are found in the southern Indian Ocean and between Australia and the date line. Note that the strongest signal in the *v*-only analysis occurred in the central Pacific north of the equator (not shown). This signal is only weakly present in the vector analysis. A final and important point, to be returned to in Part III is the occurrence of a clear equatorial minimum in the *v*-component just south of the equator in the western Pacific. Both components together show the Southern Indian Ocean to be a participant in the mid-Pacific fluctuation pattern.

The spatial phase information (Fig. 3) is represented via the spatial state vectors, i.e. $S_n e^{i\theta_n}$. The number of barbs on each vector is proportional to the spatial amplitude; the barbs essentially carry the information shown in Fig. 2. The directions of the vectors relative to the key show the sense (±) of the simultaneous fluctuations in the vector components. Finally a smooth rotation of the vectors in space represents propagation of information. Counterclockwise rotation represents eastward propagation.

The *u*-component fluctuations are broadly in phase over most of the western Pacific, central Pacific and southern Indian oceans. The variations in the equatorial and northern Indian Ocean are approximately 180° out of phase with the former regions because the state vectors are pointing in the direction opposite those in the Pacific and southern Indian Oceans. Thus, westwardly-directed anomalies in the Indian Ocean go with eastwardly-directed anomalies in the central and western Pacific. Alternatively, eastwardly-directed anomalies in the Indian Ocean go with westwardly-directed anomalies in the Pacific. This pattern of variation clearly represents the modulation of the Indonesian convergence and reproduces results described in I.

There is indication of propagation of information along the equator between Indonesia and the date line and further into the higher latitudes of the Northern Hemisphere. This is seen in the systematic counterclockwise rotation of the *u*-component state vector from Southeast Asia to the date line. Thus, in the equatorial region the results of I are largely reproduced by the current analysis. Note that the South Pacific region seems to experience basically simultaneous changes in the zonal component of the vector wind; these changes are essentially in phase

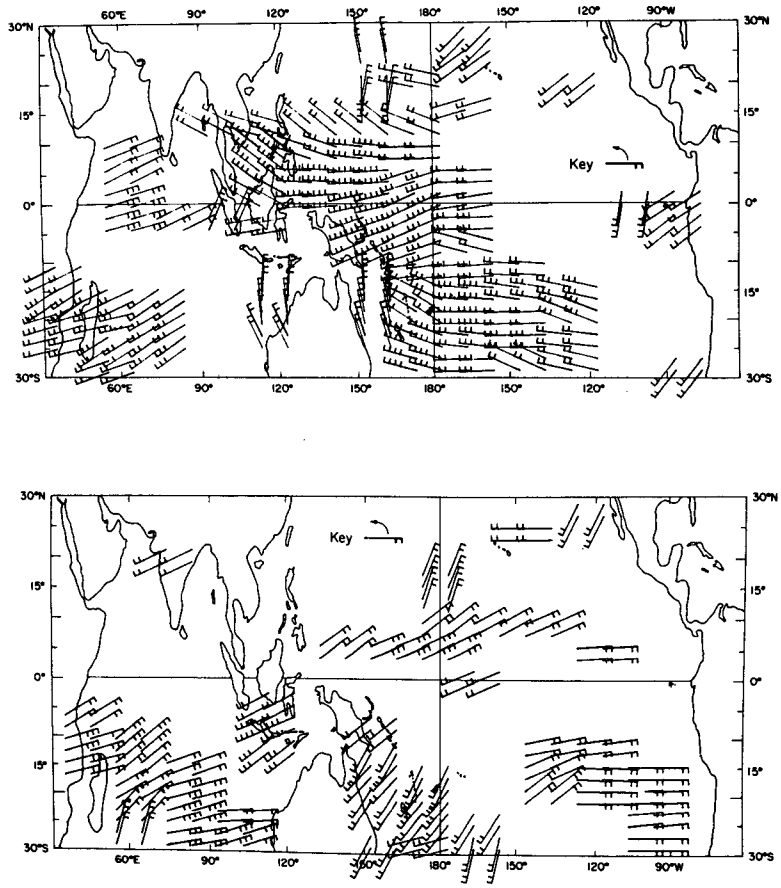

FIG. 3. Components of the spatial state vector of the anomalous vector component of the Monsoon/Trade Wind System. The number of flags indicates the magnitude of the spatial power (in relative units of 0.05). Signals with magnitudes less than 0.10 are omitted. The directions of the flags indicate the relative spatial phases of fluctuations in different regions of the fields. The phase is measured counterclockwise with respect to the positive x-axis (see key). Upper panel shows the contribution of the zonal component to the spatial state vector; lower panel shows contribution of the meridional component to the spatial state vector. See Part I, Appendix Section 3 for additional details.

with those along the equator east of Indonesia. The equatorial signal of I clearly is coupled to u-changes in the Southern Hemisphere.

The meridional components exhibit a less well-defined phase structure (Fig. 3, lower) than do the zonal flow anomalies. The variations in the southeastern Pacific, southern Indian Ocean and central Pacific north of the equator are essentially in phase with each other. From Indonesia across Australia to the dateline, however, variations in the v-component are out of phase with the regions previously mentioned. Physically, this means that northward anomalous flow over the eastern South Pacific and Indian oceans is associated with southward flow between 100°E and 170°W. The reverse holds also.

These patterns suggest the existence of two preferred spatial states for the lower-level convergence zones of the Indian/Pacific Oceans. One state is associated with enhanced convergence over the Indonesian/west Pacific; the other with enhanced convergence over the Indian and eastern Pacific Oceans. The manner in which these states vary in time is considered in the next section.

Evidence for propagation of information in the v-component is weak. The strongest systematic rotation of the state vectors occurs along the Indonesian–New Zealand axis and suggests a northwest-to-southeast flow of information.

The state vectors offer an intriguing glimpse of the interaction between the Walker and Hadley cells. Let the former be represented by zonal wind anomalies near the equator and the latter by meridional flow anomalies within, say, 20° of the equator. The Walker cell tends to have phase values of roughly 0° or 180° (ignoring propagation for the moment), since the state vectors point either east (0°) or west (180°).

The Hadley cell, on the other hand, has spatial phase values of roughly 210° north of the equator and 30° or 210° south of the equator. Since both cells are modulated in time by the same principal component $A_1(t)$, the two hypothetical circulation cells are not in quadrature as has been suggested previously. The fact that they are not in quadrature means there can be a substantial interaction between the two systems. The quantitative relation between the two cells will be clarified in Part III.

b. Temporal properties

The time variation of the spatial pattern discussed above was investigated through the first principal component, $A_1(t)$, a complex number that has both rms amplitude and temporal phase ϕ (see Section 2 and Part I). Those quantities are shown in Fig. 4. Also shown is a time series of SST anomalies for a large region of the central equatorial Pacific (180–140°W, 5°N–5°S).

The phase shown in the upper panel of Fig. 4 does *not* show the temporal bimodality seen in the Part I analysis (see Part I, Fig. 12). Such a feature is apparently a property of the near-equatorial zone only. In this analysis, the phase shows only a marginal preference for the range −90° to +90°. This range of phase values corresponds to intensified convergence (CON) over the Indonesian region, i.e. enhanced inflow from both the Pacific and Indian Oceans. Values outside this range correspond to anomalous divergence (DIV) over Indonesia. The phase generally exhibits a fairly smooth, monotonic behavior with time. This suggests that the feature of the surface wind field captured by mode 1 is a regularly occurring feature of the tropical atmosphere that waxes and wanes over the timescales of 2–7 years. The time series of ϕ_1 was highly suggestive of a frequency modulated process with parameters almost identical to those estimated in Part I. We shall return to this apparently curious result in Part III.

The temporal phase is strongly related to the SST in the central equatorial Pacific. Indeed, each phase transition from +180° to −180°, a time of maximum anomalous divergence over Indonesia, precedes a warm event in the central ocean except in 1976 (five out of six cases). These transitions occur in either the spring or the fall. Further, it is clear that anomalous convergence over Indonesia is associated broadly with colder SST than normal while anomalous divergence is related to warmer SST than normal.

Closer inspection of Fig. 4 reveals a number of disturbing facts. The temporal modulation of the Indonesian convergence is not very well related to SST in the central ocean. For instance, the atmospheric system goes from anomalous divergence to convergence and back to divergence while the anomalous SST a) remains negative but essentially unchanged (1954–56); b) is essentially zero (1959–62). Similarly, the vergence transition can either occur while the ocean remains warm (1969) or simply not be evident in the data set ($\phi = \pi/2$) during a major warm event (1976–77). In summary, the atmosphere seems to have a mind of its own: although there is a rough correspondence between atmospheric state and central Pacific SST, the strong cause-and-effect relationship often envisioned is hard to see in this analysis.

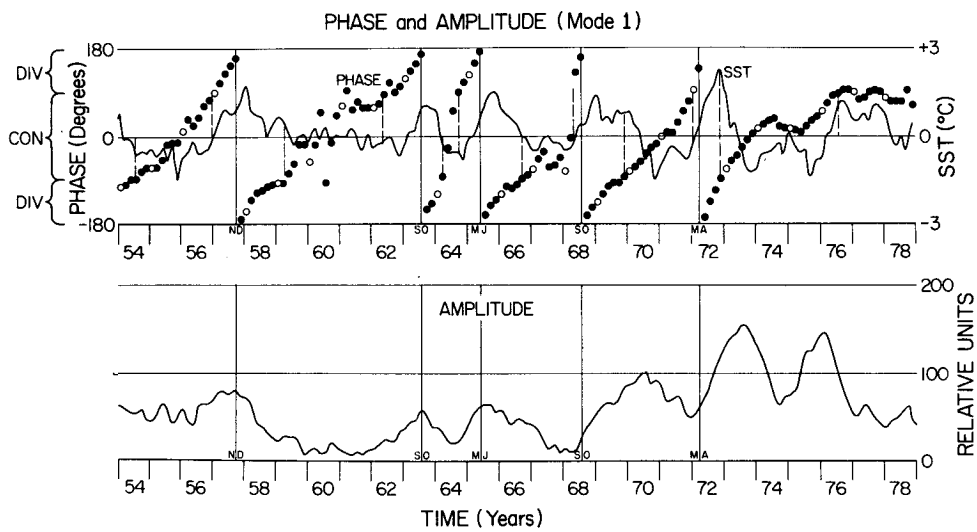

FIG. 4. Time-dependent properties for mode 1 of the vector-wind analysis. Upper panel shows temporal phase (dots) and central Pacific SST anomaly series. Solid vertical lines indicate $+\pi/-\pi$ phase transition; letters indicate the bimonth of transition. The heavy dashed lines denote phase value of $\pm\pi/2$, the transition between anomalous convergence/divergence over Indonesia. Open circles denote the January–February bimonth. Lower panel shows temporal amplitude function.

The rms amplitude of the mode 1 vector wind anomalies (Fig. 4, lower) is not well-related to the SST signal. Indeed the largest values (April 1973 and January 1976), occur at times of small, slightly negative SST anomaly in the central ocean. The same situation occurs in 1970. By contrast, the weak peaks in 1957, 1963 and 1965 occur during times of maximum relative divergence and are associated with an SST warming but precede the maximum warming by several months. Finally, the warm SST event of 1968–69 does not appear in the rms amplitude data as a distinct event.

The above results broadly agree with those of earlier works (Bjerknes, 1966; Rasmusson and Carpenter, 1982; Horel, 1982 and others) in that a warmer-than-normal central equatorial Pacific goes with anomalous divergence over Indonesia and, similarly, with reversal of the anomaly signs.

The results do not agree well, however, regarding the temporal evolution of the divergence–SST relationship. Similarly, modeling results (Shukla and Wallace, 1983; Keshavamurty, 1982, and others) would suggest a nearly one-to-one correspondence between SST anomaly evolution and wind field change. Clearly, this situation is not apparent in Fig. 4. Evidently, the idea that El Niño–Southern Oscillation events conform to a consistent set of rules may need some revision.

The above dichotomy will be resolved in Part III, where it will be shown that the wind patterns discussed herein are but one part of a near-global climatic signal of which "local" Pacific climate variations (El Niño, etc.) are just one part. Thus, the authors mentioned above, and many others, have been examining a "local" signal whereas the current study has uncovered a climatic variation of near-global dimension. The two signals do not bear the same relation to the central Pacific SST, nor should they necessarily be expected to.

c. *Reconstructed flow field*

The above results are brought to life via a reconstruction of mode 1 keyed to the warm/cold SST events of the early 1970s (Fig. 5). The temporal amplitude/phase for these reconstructions is nearly identical to those associated with the summer monsoon period (bimonth 4) so the result shown in Fig. 5 can be thought of as being keyed to that climatic feature as well (at least for this particular case).

The September–October 1971 period, with temporal phase near 0°, shows strong anomalous *convergence* over Indonesia and along the east Australian coast. Anomalous cross-equatorial flow from south to north also exists. The summer monsoon is strong and confined mainly to the Indian Ocean. The easterlies in the western halves of the South Indian and South Pacific are also strong, with the Pacific winds penetrating along the equator to Indonesia. There is substantial meridional flow in the eastern halves of both oceans.

By January–February (middle panel), the sense of the vector anomaly field has shifted to its "El Niño mode" whence it will rapidly intensify in time. The anomalous *divergence* over Indonesia, a telltale sign of events to come, is in place as found also in Part I. The easterlies have weakened over a broad latitudinal expanse near the date line. The winter monsoon is weaker than usual. From Fig. 4 it is clear that SST in the central ocean is still below normal.

By September–October 1972 (Fig. 5, lower panel), the height of the ocean warming has just occurred off South America, the wind field temporal phase has just shifted phase through π and, therefore, is starting to return to its "cold mode." These first hints of recovery are visible in the westward anomalies off eastern Australia and in the increased anomalous convergence over Indonesia. In the equatorial regions the wind system is yet unchanged, being still in its warm phase. Strong anomalous convergence exists near the date line, while the summer monsoon is weak but has expanded its region of influence to cover the western equatorial Pacific.

The main changes, relative to the seasonal cycle, are clearly in the western equatorial Pacific followed by the Indian Ocean and southwest flank of the northeasterlies. Other changes appear as subtle shifts in both wind direction and speed. In general, the signal that is being discussed is of the order of 20% of the magnitude of the mean seasonal wind with obvious exceptions in the Indonesian region, where the anomalies can exceed the seasonal signal.

4. Conclusions

Examination of the space/time scales of the Monsoon/Trade Wind Systems between ±30° latitude has been carried out with a sophisticated filtering analysis (complex EOFs) designed to investigate the largest spatial scales of variability. The method can detect simple moving features in the data field if they are present. This study (Part II) complements earlier analyses of these same wind fields in the band ±10° of the equator (Part I) and sets the stage for a physical, synoptic examination of the results of I and II.

The principal results of this study were as follows:

a) Increasing the domain of analysis gave many of the same results as were found in Part I. This suggests that the results are largely immune to EOF-domain effects (Buell, 1979). The differences that did occur were associated with variability in the additional data. Increasing the domain to include higher latitudes also reduced the signal-to-noise level of the analysis, as might be expected. The features to be discussed below are weak compared to the total variability, about 10–20% of the variance on average. However, the prin-

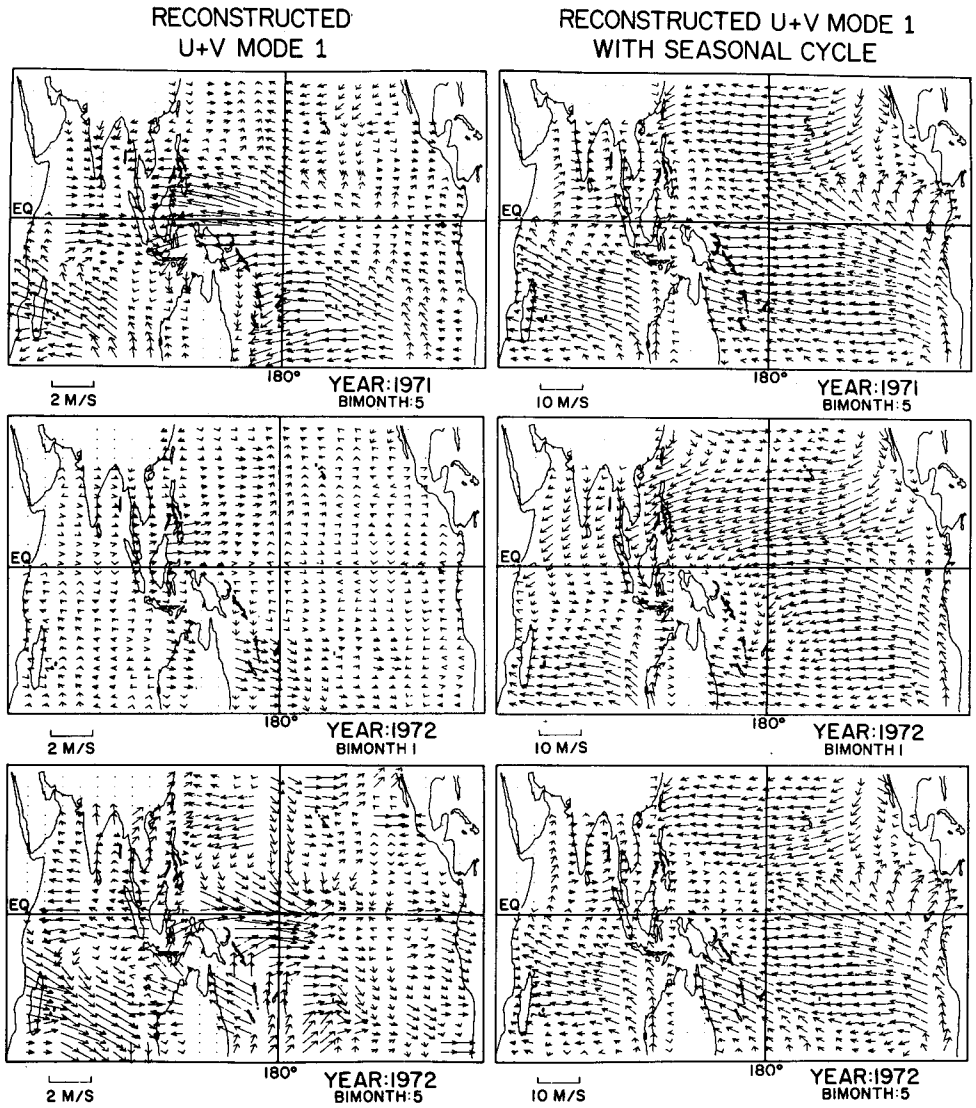

FIG. 5. Left panels show reconstruction of the vector anomaly field associated with mode 1; right panels show the sum of the anomaly and long-term mean fields.

cipal patterns are sometimes strong enough (64% of the field variance) to be seen in the raw data, thus supporting their occurrence in nature.

b) The Monsoon/Trade Wind fields are strongly coupled to each other and to variability in the tropical latitudes of the Southern Hemisphere on a massive scale. A weaker coupling to the Northern Hemisphere was evident along the coast of Asia and in the central Pacific. A far stronger coupling is the large North–South transfer of mass that takes place over the surface of the Indian Ocean. Thus, the pulsation of the huge Indonesian convergence zone, plus the establishment (found in Part I) of a central equatorial Pacific convergence near the date line, are seen to be but one part of a larger set of global climatic variations.

c) The apparent *propagation of information* found in Part I (from Indonesia along the equator to the central Pacific via the zonal flow) is still apparent. However, this event is accompanied by fluctuations at higher latitude, particularly in the Southern Hemisphere. The region of the South Pacific convergence zone (SPCZ) seems to be a breeding ground for such perturbations, but the coastal region of Asia may be a source area also.

d) The apparent bimodal vector wind state found in Part I is not apparent in the current analysis. The vector anomaly field in this study showed only a small preference for any one distribution of wind anomalies; this distribution of wind was generally associated with cool water in the eastern and central equatorial Pacific and with anomalous convergence over Indonesia.

e) The meridional wind anomalies weaken and strengthen almost simultaneously over the central

Pacific. However, the modulation is of reverse sign between the North and South Pacific. The result represents, to first order, a massive modulation of the equatorial convergence (Hadley cell) over the Pacific.

f) The pattern of variation seen in the Monsoon/Trade Wind field corresponds only broadly with the evolution of the anomalous SST in the central Pacific. There appears to be numerous discrepancies in the idea that the SST anomalies alone can account for the observed variations in atmospheric behavior. This result is explored in more depth in Part III; for now it is concluded that the wind field variations described here are but one part of a larger, near-global mode of climatic variations that may be forced by mechanisms other than those associated with Pacific SSTs.

Acknowledgments. Leonid Volfson carried out the calculations and produced the graphics. Grace Johnston transcribed the manuscript. The computer work on the data aspects of the problem was carried out by Tony Tubbs and Peter Crill. Sincere appreciation is also due K. Hasselmann of the Max Planck Institute, Hamburg, for the quiet time needed to prepare this manuscript. The author gratefully acknowledges the support of the Climate Dynamics Office of the National Science Foundation (Grants ATM-7918206 and ATM-8213279). The detailed comments, views and suggestions of an anonymous reviewer and Kevin Trenberth substantially improved the manuscript and are gladly acknowledged.

REFERENCES

Barnett, T. P., 1977: An attempt to verify some theories of El Niño. *J. Phys. Oceanogr.*, **7**, 633–647.

——, 1983: Interaction of the monsoon and Pacific Trade wind system at interannual time scales. Part I: The equatorial band. *Mon. Wea. Rev.*, **111**, 756–773.

——, 1984: Interaction of the monsoon and Pacific trade wind system at interannual time scales. Part III: A partial anatomy of the Southern Oscillation. *Mon. Wea. Rev.*, **112**, 2388–2400.

Bjerknes, J., 1966: A possible response of the atmospheric Hadley circulation to equatorial anomalies of ocean temperature. *Tellus*, **18**, 820–829.

Buell, C. E., 1979: On the physical interpretation of empirical orthogonal functions. *Preprints Sixth Conf. Probability and Statistics in Atmospheric Sciences*, Banff, Amer. Meteor. Soc., 112–117.

Horel, J., 1982: On the annual and interannual variations of the tropical Pacific atmosphere and ocean. Ph.D. Dissertation, University of Washington, 121 pp.

Keshavamurty, R. N., 1982: Response of the atmosphere to sea surface temperature anomalies over the equatorial Pacific and the teleconnections of the Southern Oscillation. *J. Atmos. Sci.*, **39**, 1241–1259.

North, G. R., T. L. Bell, R. F. Calahan and F. J. Moeng, 1982: Sampling errors in the estimation of empirical orthogonal functions. *Mon. Wea. Rev.*, **110**, 699–706.

Preisendorfer, R. W., F. W. Zwiers and T. P. Barnett, 1981: Foundations of principal component selection rules. SIO Ref. Ser. 81-4, Scripps Institution of Oceanography, University of California, 192 pp.

Shukla, J., and J. M. Wallace, 1983: Numerical simulation of the atmospheric response to equatorial Pacific sea surface temperature anomalies. *J. Atmos. Sci.*, **40**, 1613–1630.

Rasmusson, E. N., and T. H. Carpenter, 1982: Variations in tropical sea surface temperature and surface wind fields associated with the Southern Oscillation/El Niño. *Mon. Wea. Rev.*, **110**, 354–383.

Wyrtki, K., and G. Meyers, 1975: The Trade Wind field over the Pacific Ocean, Part I, The mean field and the mean annual variations. Hawaii Institute of Geophysics, University of Hawaii, HI, 1–25.